GPS Pseudorange Simulator

Summary of dissertation for the degree of Master in Telecommunications and Informatics Engineering

Sílvia Maria Urmal de Almeida
Instituto Superior Técnico, Technical University of Lisbon, Portugal
silvia.almeida@tecnico.ulisboa.pt

ABSTRACT

With the evolution of the technology related to GPS receivers, it is necessary to test their performance. To do so, simulators are implemented whose aim is to assist the development of more efficient receivers and test positioning and navigation algorithms.

This work aims to create a GPS pseudorange simulator for users of the SPS service. This simulator's purpose is to produce pseudoranges similar to those that would be obtained between a given GPS receiver and several satellites.

In order for the pseudoranges to be as realistic as possible, it is essential to take into account the various error sources that affect the measurements, besides the receiver's clock's bias. These error sources may originate from various segments of the GPS. While in the control and space segments the error sources are delays related to the satellite clocks, inter-signal delays and errors related to the ephemeris broadcast, in the user segment the errors are associated to atmospheric delays, the receiver noise and multipath.

After the simulator has been implemented, the DOPs and the errors in the estimations of the receiver's position and clock's bias must be calculated so that conclusions can be drawn about its performance.

Keywords

Simulator; Pseudoranges; GPS; Error Sources.

1. INTRODUCTION

1.1. INTRODUCTION

This project consists in developing a GNSS (Global Navigation Satellite System) GPS (Global Positioning System) pseudorange simulator for SPS (Standard Positioning Service) users, i.e. for users whose receivers are single frequency (L1 C/A), in order to be used in the production of tests on the performance of positioning and navigation algorithms.
The simulator will use real orbital parameters of the GPS system and must take into account the sources of error that typically affect pseudorange measurements. Models will be implemented to compensate for ionospheric, tropospheric and clock (both receiver and satellite) delays.
A website will also be built so that the user has an interface with which to interact with the simulator, giving inputs and then be able to view the simulator results.
The efficiency of the simulator will be validated by using the pseudoranges resulting from the simulator to estimate the receiver's position and the deviation of its clock and compare the estimates with the data given by the user as input.

1.2. STATE OF THE ART

Numerous GNSS simulators exist on the market [1][2]. Many of these simulators aim to provide solutions for research, test production and development of receivers for various GNSS such as GPS, GLONASS (Globalnaya Navigatsionnaya Sputnikovaya Sistema), Galileo, among others.
These simulators are composed of software programs and are often accompanied by hardware devices.
GNSS simulators can be characterized in several ways according to the functionalities they offer, such as being able to simulate satellite constellations and their signals. The GNSS High Fidelity: Constellator simulator from Syntony [2] is one of these simulators. It is capable of reproducing multiple signals for all available satellite constellations, operates with several frequencies as well as with only one and uses several models (ionospheric, Earth gravity, etc.). It also offers the possibility of performing simulations for various types of orbits such as LEO (Low Earth Orbit), MEO (Medium Earth Orbit), GEO (Geostationay Earth Orbit), etc. In this way, it is possible to reproduce the most varied scenarios according to the user's preference.
Another company that provides GPS/GNSS test devices is Spirent Federal. An example of equipment it offers is the GSS9000 [2]. This solution aims to

provide its user with the opportunity to test navigation systems using various constellations of not only different GNSS but also regional navigation systems. This simulator also allows testing using various codes, including codes restricted to civilian use. In this way, users are able to create various test scenarios so that they can analyse and draw conclusions about the performance of the most varied navigation systems.

There are other simulator models whose features are even more advanced and complex compared to the models previously described, such as the QA707 GNSS and Interference Software Simulator [1] from QASCOM company. This solution allows testing various types of interference and cyber-attacks to GNSS, allowing the simulation of numerous attack scenarios.

This work takes as inspiration devices like the ones mentioned above. However, this work will be simpler in that the proposed solution is software-only based, it takes only into account GNSS GPS and operates exclusively for SPS users.

2. THEORETICAL CONCEPTS

2.1. GPS

In the early 1970s, the United States Department of Defense launched a new project, NAVSTAR-GPS (Navigation System with Timing and Ranging - Global Positioning System). This system aims to provide global positioning and navigation services regardless of weather conditions and at any time of day. Initially, this system was only available for North American military purposes. In the 1980s, its availability was expanded also for civilian purposes [3][4].

2.2. GPS System Architecture

The GPS system can be characterized into 3 distinct segments [5]:

Space Segment

This segment consists of a nominal constellation of 24 satellites orbiting the Earth in 6 orbital planes. These orbital planes are at a distance of 60° from each other and have an inclination of 55° with respect to the equatorial plane. These satellites take approximately 12 hours to complete one orbit around the Earth. In order for them to complete one circle in 12 hours, the satellites travel at altitudes close to 20200 km. Any GPS receiver is capable of receiving signals from at least 4 satellites at any instant of time and at any point on Earth [5].

Control Segment

As the name suggests, the control segment has the function of controlling the entire GPS system. The control segment is composed of 5 ground stations distributed around the world in locations that allow the monitoring of all satellites during 92% of the time. This segment collects informationabout the constellation of satellites previously described, namely about their health, orbits and precision of their clocks. This information, collected by all stations, is then sent to the main control station in Colorado Springs in the United States. At this station, the data is processed and ephemerides and satellite clock corrections are calculated. Then, messages with control data are sent to each satellite, through one of the 3 uplink stations [5].

User Segment

This segment consists of the use of the GPS receivers by the users of the system. Depending on the purpose for which the GPS receivers are used, they are configured in different ways. The GPS receivers can have as applications the terrestrial, maritime and aerial navigation, surveillance, cartography, among others. Depending on the receiver application, it uses different algorithms in the processing of the data to which it has access, such as pseudodistances [5].

2.3. GPS Services

GPS offers two distinct categories of positioning services, the *Precise Positioning Service* (PPS) and the *Standard Positioning Service* (SPS). While PPS is only available to authorized users such as the US military, allies and the US government, SPS is also available to civilian users [4][5].

2.4. Position of the Satellites

It is important to calculate the position of a given satellite, using the orbital parameters that characterize its orbit, since this information is essential for the acquisition of the position of a given receiver. IS-GPS-200 can explain how this calculations are achieved [6].

2.5. Pseudoranges

The pseudoranges are relevant to obtain the location of the GPS receivers since they need at least four of these measurements to estimate their position. The pseudoranges can be represented by equations (1) and (Erro! Utilize o separador Base para aplicar 0 ao texto que pretende que apareça aqui.**2**), where $c\Delta tr$ (m) is the distance from the clock offset of the receiver s=(xs,ys,zs) are the ECEF Cartesian coordinates in metres for a given satellite, and r=(xr,yr,zr) are the ECEF Cartesian coordinates in meters for a given receiver [7].

	$\rho = \sqrt{(x_s - x_r)^2 + (y_s - y_r)^2 + (z_s - z_r)^2} + c\Delta t_r$	**(1)**
	$\rho = \|s - r\| + c\Delta t_r$	**(**Erro! Utilize

		o separador Base para aplicar 0 ao texto o que pretende que apareça aqui .**2)**

These pseudoranges are, however, noiseless which is not the case in reality. It is also necessary to take into account other effects that disturb the GPS signal and introduce noise to the measurements. These sources of error are varied, for example, the error of the satellite clocks $\Delta ts(s)$atmospheric effects such as tropospheric $\Delta ttropo(s)$ and ionospheric $\Delta tiono(s)$ etc. Equation (3) is intended to represent pseudodistances that take into account some of these error sources [8].

	$\rho = \|s - r\| + c\Delta t_r + c\Delta t_s + c\Delta t_{tropo} + c\Delta t_{iono} + \cdots$	**(3)**

2.6. Error Sources

2.6.1. Pseudorange Error Budget

There are numerous error sources that affect the pseudodistance measurements. It can be seen from the analysis of Table 1 that in the control and space segments, the sources of error are deviations in the broadcast clocks, the group delay L1 P(Y) - L1 C/A and the error in the ephemeris broadcast. On the other hand, the error sources coming from the user segment are the ionospheric and tropospheric delays, the receiver noise and multipath [8].
It is assumed that, through a normal distribution with null mean and standard deviation (m) characteristic of each error source, it is possible to design a random variable in meters representative of the error of each parameter. These random variables aim not only to simulate the random aspect that each component has in the pseudodistance measurements but also to compensate for any residual errors [5][8].
Analysing Table 1, it can be seen that the ionospheric delay is by far the error source contributing most to the uncertainty of the measurements, with a standard deviation of 7 m, followed by the satellite clock delay whose standard deviation is 1.1 m. It is concluded that, even using models that try to remove these errors, some residual errors prevail [5].
The uncertainty of the pseudodistance measurements for each satellite is called UERE (User Equivalent Range Error) [8].

Table 1 - GPS SPS UERE Budget [8]

Segment source	Error Source	1σ Error (m)
Control/Space	Broadcast clock	1.1
	L1 P(Y) - L1 C/A group delay	0.3
	Broadcast ephemeris	0.8
User	Ionospheric delay	7.0
	Tropospheric delay	0.2
	Receiver noise and resolution	0.1
	Multipath	0.2
System UERE	Total (RSS)	7.1

2.6.2. Satellite Clock Error

When creating a pseudorange simulator, the time offset of the satellite clocks $\Delta ts\,(s)$ with respect to the GPS system time must be taken into account. The satellite clocks may result in deviations that can reach values of up to 1 ms [8].

2.6.3. Group Delay L1 P(Y) - L1 C/A

Another correction parameter is the inter-signal correction $ISCL1C/A\,(s)$ which aims to eliminate the delay between L1 P(Y) and L1 C/A codes [6].

2.6.4. Broadcast Ephemeris Error

This error source comes from disparities between the orbital parameters transmitted in the ephemeris and

the real orbits of the satellites. This happens because there are forces, in addition to the gravitational force of the Earth, which influence the orbits of the satellites, making it difficult for the Control Segment to parameterize them [9].

2.6.5. Atmospheric Effects

The Earth's atmosphere can be divided into several layers. In this context, however, we work with only two, the ionosphere and the troposphere. Each of these layers is characterized by different phenomena that occur in it [10].

Both ionospheric and tropospheric delays result from the fact that signals change their propagation medium when passing through the atmosphere, thus delaying their propagation speeds and changing their trajectory [5][8][10].
The ionospheric delay may be compensated by utilizing the Klobuchar model [6].
There are multiple models that aim to compensate for the delay of GPS signals introduced by the troposphere. Two examples are the Hopfield model and the University of New Brunswick tropospheric model 3 (UNB3) [8][11].

2.6.6. Receiver Noise and Resolution

This error source is associated with the thermal noise of the GPS receiver [12]. The thermal noise results from small variations in a given electrical current, in this specific case, the receiver's electrical current [13].

2.6.7. Multipath

As the name implies, multipath is a phenomenon that consists in receiving the same signal several times, because it reaches the receiver through multiple propagation paths. This effect is caused by the presence of reflective surfaces such as buildings, trees, etc. that are near the receiver and cause the signal to be reflected. [3][10].

2.7. GPS satellite receiver position estimation

Pseudoranges consist of distances from a given receiver to the satellites along with the distances from the delays that the GPS signal will experience during its journey between the satellites and the receiver. Assuming that the receiver's clock's deviation from the GPS system time - one of the error sources that affect the pseudoranges- also affects all the measurements of the satellites' pseudoranges, it is possible to estimate the receiver's position using information from at least four satellites [5]. The minimum number of satellites sending information must be four since the receivers have to calculate the values of 4 unknowns: the latitude, longitude, altitude, and the deviation of their clocks [7].

2.7.1. Least-Squares Algorithm

An algorithm to obtain the position estimate of a given receiver is least-squares [5][14] based on pseudorange measurements.

2.7.2. DOPs (Dilution of Precision)

The geometry of the visible satellites around the position of a receiver at a given time instant will influence the results of the receiver's position estimation. The DOP (Dilution of Precision) parameters allow assessing this geometry [8][10].

As the name of these parameters indicates, the accuracy of the position estimation is diluted when the geometry of the satellites is not favorable. The higher the value of DOP, the greater the error in the accuracy with which the estimates of the positions are made [8][10].

3. SIMULATOR DEVELOPMENT

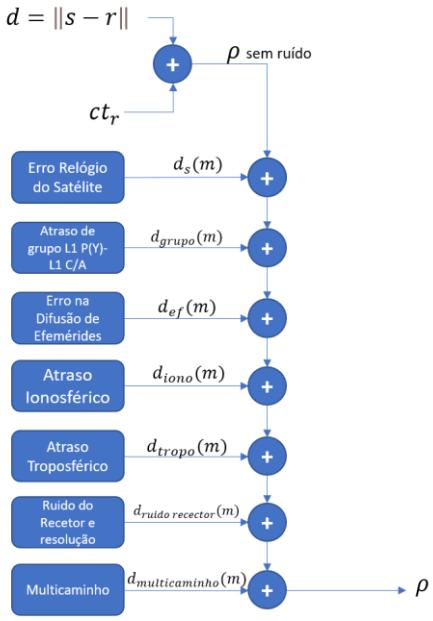

Fig. 1 - Simulator architecture

This simulator was realized through several MATLAB scripts that interact with each other and use information from several files with data.
Firstly, the user is asked to enter the Cartesian coordinates of the receiver location and the offset and rate of the receiver clock offset.
The user has the opportunity to control the value of the minimum elevation, in relation to a given range of azimuth angles chosen by the user, for which the pseudorange measurements are made. By manipulating these parameters, the user can simulate

situations where a given GPS receiver is in places where there may be obstacles in the passage of the GPS signal, such as the existence of buildings in the vicinity. In this way, the user controls the direction and elevation of the GPS signals to which the simulator will return the pseudorange measurements.
The user provides the simulator with the initial and final TOW and WN as well as the rate (every 2 seconds, for example) for which they want the pseudorange measurements.
The user can decide to submit his own RINEX navigation message file as input to the simulator.
On the other hand, the user can choose not to provide the RINEX file and the simulator will extract the file online from the IGS CDDIS data center compatible with the WN and TOW previously provided. The collection of RINEX also depends on the receiver position chosen, and the files can originate from stations in Canada or the Philippines. In this way, the simulator can ensure that the ephemerides that are used in the calculations are valid and that there are several satellites visible for many points on the globe.
The data file is then read. The orbital parameters in the file are used to determine the positions of the various satellites in the file.
The ionospheric delay is given by the output of the Klobuchar model, for which it is necessary to provide ionospheric correction parameters from the RINEX navigation message file. The clock delay of the satellites is calculated correction parameters from the data file mentioned above. To obtain the errors of these parameters in terms of distances, it is necessary to multiply these delays by the speed of light.
The user will then be asked to choose between the two tropospheric models available, the UNB3 model or the Hopfield model. Depending on their choice, the user will be asked to enter some data regarding the selected model. Both the UNB3 and the Hopfield models give as output the tropospheric error in meters.
Each of these errors was simulated using random variables of normal distribution.
The multipath error is simulated through a random variable acquired through a normal distribution with null mean and standard deviation acquired.through Table 1. The same procedure is done for the receiver noise and resolution, the error in the ephemeris diffusion and the L1 P(Y) - L1 C/A group delay. It should be noted that the user can also choose to change the standard deviation used in the creation of the random variables previously mentioned.
From this information, the pseudoranges of the satellites are calculated, in a given time interval, at a given rate. As shown in Fig. 1, each pseudorange is calculated by adding the distances from each error source, including the distance from the clock offset of the receiver, to the distance between the satellite and the receiver. Finally, the RINEX observation data files with the pseudoranges are created and displayed to the user.

4. EVALUATION

After the pseudoranges are processed, the least-squares algorithm is applied, which estimates the position and deviation of the GPS receiver clock for several time instants.
The DOP parameter values are also calculated, which allow conclusions to be drawn about the effect that satellite geometry has on the accuracy with which the position and clock offset of the receptor are estimated.

1st Scenario

In this scenario, several graphs were created and analysed according to the input data explained in the following tables.

Table 2 - data referring to the receiver

Latitude (°)	38.7377
Longitude (°)	− 9.1385
Altitude (m)	199.5442
Clock Offset (μs)	500
Clock Drift (μs)	0.4

Table 3 - Azimuth and elevation mask

Azimuth (°)	Elevation (°)
From 0 to 9	5
From 10 to 149	10
From 150 to 299	5
From 300 to 360	20

Table 4 - TOWs, WNs and rhythm

Initial TOW (s)	213984
Final TOW (s)	217584
Initial WN	2149
Final WN	2149
Measurement rhythm (s)	1

Table 5 - Random variables errors

$\sigma_{relógio\ do\ satélite}\ (m)$	1.1
$\sigma_{atraso\ de\ grupo}\ (m)$	0.3
$\sigma_{difusão\ das\ efemérides}\ (m)$	0.8

$\sigma_{atraso\ ionosférico}\ (m)$	7.0
$\sigma_{atraso\ troposférico}\ (m)$	0.2
$\sigma_{ruído\ do\ recetor}\ (m)$	0.1
$\sigma_{multicaminho}\ (m)$	0.2

In this scenario, the tropospheric delay was simulated using the UNB3 model and the day of the year chosen as input was day 68. It is also important to note that in this case, the simulator searches and uses the RINEX navigation message file through the receiver position and the TOWs and WNs given as input.

It is possible to observe in Fig. 2 the graph relating the time in seconds with the errors between the true position of the receiver and the estimates of the position that have been made.

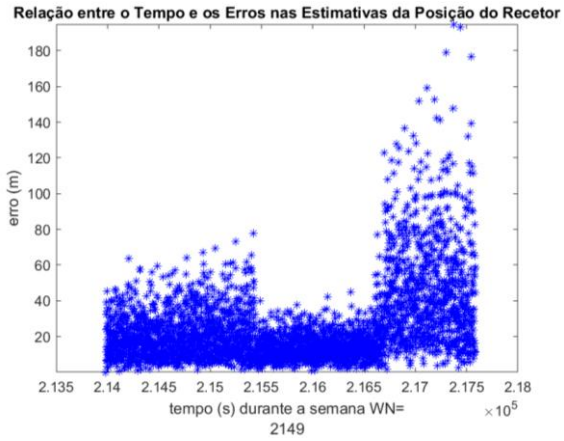

Fig. 2 - Graph of errors in receiver position estimates over time

It is possible to conclude, through the visualization of Fig. 2, that the errors are mostly concentrated in values between 0 and 30 meters, reaching, values of 190 meters.

The least-squares algorithm also allows the user to obtain estimates of the receiver clock drift. Fig. 3 shows the graph relating the time in seconds with the errors between the true receiver clock offset and the receiver clock offset estimates.

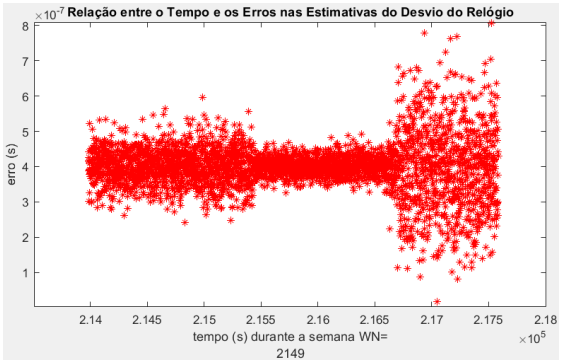

Fig. 3 - Graph of the errors in the estimates of the receiver clock drift over time

In this case, the errors in the receiver clock offset estimates are considerably larger compared to the values of the errors in the receiver position estimates. Errors in estimates of receiver clock offset are comprised in values between 3×10^{-7} and 5×10^{-7}seconds, with time intervals in which these values can range from 0 to 8×10^{-7} seconds.

The various DOP parameters pertaining to the satellite constellations for each time instant are also calculated.

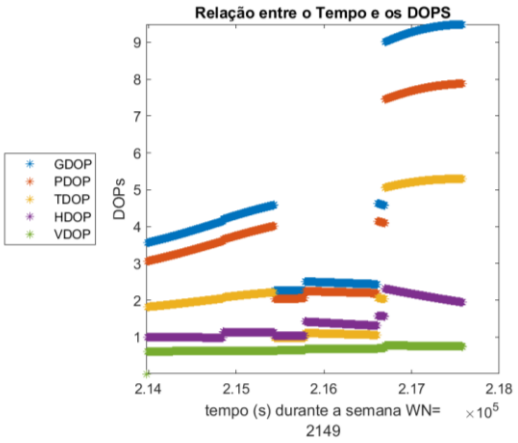

Fig. 4 - *Graph of DOP values over time*

Analysing the DOP plot in Fig. 4, in the time interval of between approximately TOW=215500 s and TOW=216900 s, the values of the GDOP, PDOP and TDOP parameters are the smallest which indicates a better geometry of the constellation satellites during this time interval. Thus, the errors of the receiver position and clock drift estimates are concentrated in more specific values, as it is possible to see in Fig. 2 and Fig. 3.

On the other hand, it is concluded that in the last moments, between about TOW=216900 s and TOW=217584 s, the values of the GDOP, PDOP and TDOP parameters increase considerably, which allows one to infer that the geometry of the satellites is worse during this time interval. This worsening is also reflected in the estimate of the position and clock offset of the receiver, with a greater dispersion of the values of errors in the estimates during this time interval, as can be seen in Fig. 2 and Fig. 3.

In addition to the errors in the receiver position estimates, the receiver clock offset and the calculation of the DOPs over time, it is also possible to observe the evolution of the pseudoranges of each satellite over time, as Fig. 5 indicates.

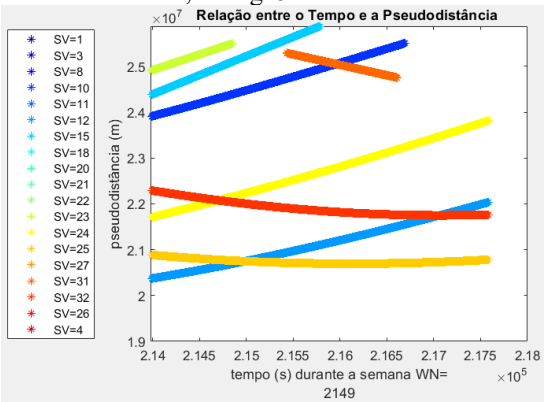

Fig. 5 - ***Graph of the pseudodistances for each satellite over time***

It was also created a graph that indicates which satellites are visible to the user for each instant of time. Analysing Fig. 6, it's observed that not all satellites are visible at the same time, existing, however, a minimum of 4 visible satellites, ensuring, in this way, that it is always possible to estimate the receiver's position and the deviation of its clock. However, if the user chooses much higher minimum elevations for the mask, there is a risk of time instants for which there are less than 4 satellites visible. In that case, it would then be impossible to estimate the receiver's position and clock offset.

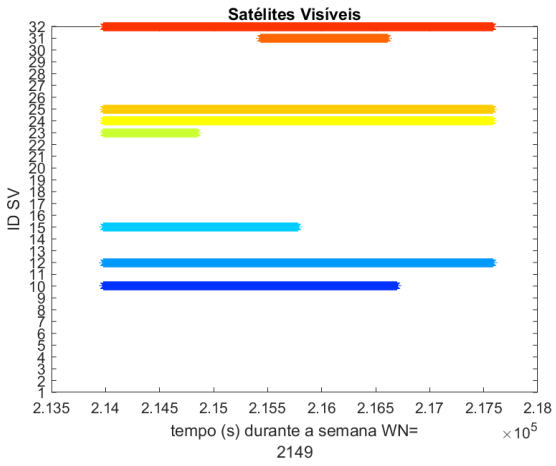

Fig. 6 - Graph of visible satellites over time

By analysing Fig. 6, it is possible to observe that for the time interval between approximately TOW=216900 s e TOW=217584 s, the number of satellites visible to the receiver is 4. In Fig. 4, the values of GDOP, PDOP and TDOP increase greatly for that same instant of time, which indicates that the geometry of the 4 satellites is not favourable.

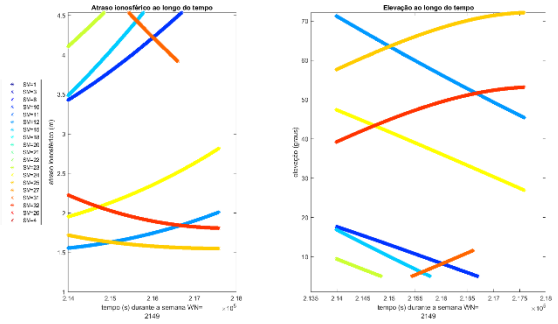

Fig. 7 - Plots of the ionospheric delay and elevations for each satellite over time

Comparing the values of the ionospheric delays of each satellite with the corresponding values of the elevations, in Fig. 7 it is observed that as the elevations of the satellites decrease, the ionospheric delays increment.

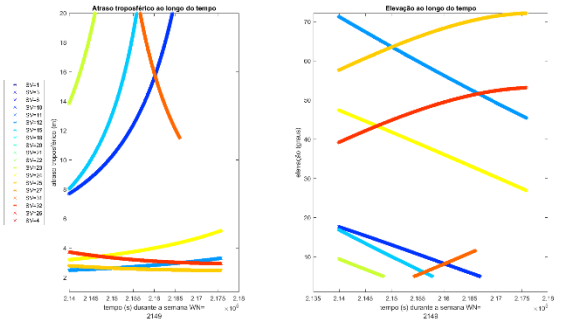

Fig. 8 - Graphs of tropospheric delay and elevations for each satellite over time

Analyzing Fig. 7 and comparing it with Fig. 8, it is concluded that the tropospheric and ionospheric delays evolve in a similar way. As the elevation of a given satellite increases, the value of the corresponding tropospheric delay decreases. The opposite also happens, that is, as the elevation of a given satellite decreases, the tropospheric delay tends to increase.

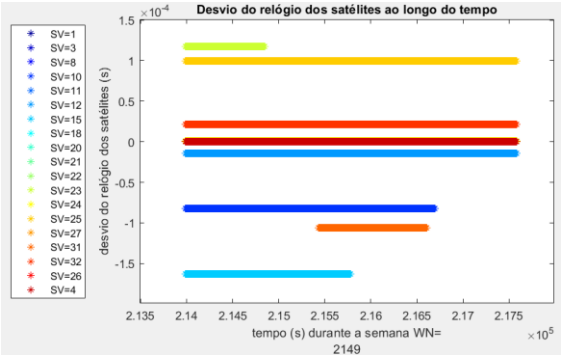

Fig. 9 - ***Graph of the clock drift of the satellites over time***

Since the clock delay of a given satellite is not dependent on its position in the orbit relative to the position of the receiver, its value is constant over time, as can be seen in the graph of Fig. 9.

2nd Scenario - Alteration in the Deviations of Random Variables

In this simulator validation scenario, several graphics were created and analyzed according to the input data explained in the following tables. In this case, the values of the deviations of the random variables in Table 6 Table 6 - Random variables were changed.

Table 6 - Random variables deviations

$\sigma_{relógio\ do\ satélite}\ (m)$	2.0
$\sigma_{atraso\ de\ grupo}\ (m)$	1.0
$\sigma_{difusão\ das\ efemérides}\ (m)$	1.0
$\sigma_{atraso\ ionosférico}\ (m)$	11.0
$\sigma_{atraso\ troposférico}\ (m)$	1.0
$\sigma_{ruído\ do\ recetor}\ (m)$	1.0
$\sigma_{multicaminho}\ (m)$	1.0

In this scenario, the tropospheric delay was simulated using the UNB3 model and the day of the year chosen as input was day 68. It is also important to note that in this case, the simulator searches and uses the RINEX navigation message file through the receiver position and the TOWs and WNs given as input.

This scenario, in comparison with the first one, has the particularity that the deviations of the random variables, used by the simulator in order to simulate the noise in the pseudodistances, have larger values. Fig. 10 and Fig. 11 illustrate the graphs relating the time (s) with the errors in the receiver position and clock offset estimates in this test scenario.

Analysing these figures and comparing them with Fig. 2 and Fig. 3 from the previous scenario, it can be seen that in this case the errors of the estimates reach much higher values. The errors in the estimates of the receiver position reach values up to 300 meters. The same happens with the errors in the estimates of the receiver clock offset, which exceed 9×10−7 seconds.

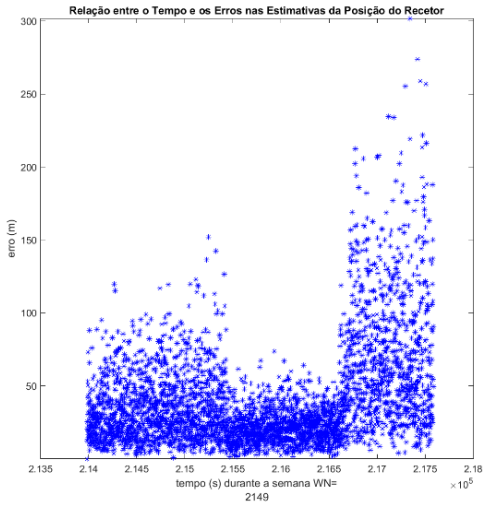

Fig. 10 - Graph of errors in receiver position estimates over time

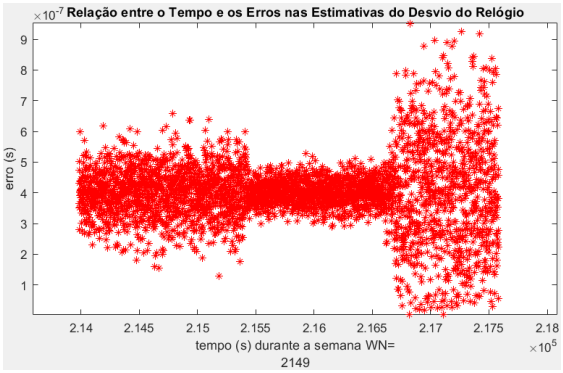

Fig. 11 - Graph of the errors in the estimates of the receiver clock drift over time

It can be concluded that, as in this scenario the pseudodistances are noisier, the receiver position and clock offset estimates have errors with larger and more scattered values.

3rd Scenario - Change of Receiver Position

In this simulator validation scenario, several graphics were created and analyzed according to the *input* data explained in the following tables. In this case, the coordinates of the receiver position in Table 7 were changed in relation to the values of the first scenario.

Table 7 - data referring to the receiver

Latitude (°)	40
Longitude (°)	130
Altitude (m)	200
Clock Offset (μs)	500
Clock Drift (μs)	0.4

Analyzing Fig. 12, it can be seen that the number of visible satellites and their IDs are different from those presented in the previous scenarios.

This phenomenon can be explained by the fact that the receiver is in another position and therefore the

pseudodistance simulator receives orbital data from another station.

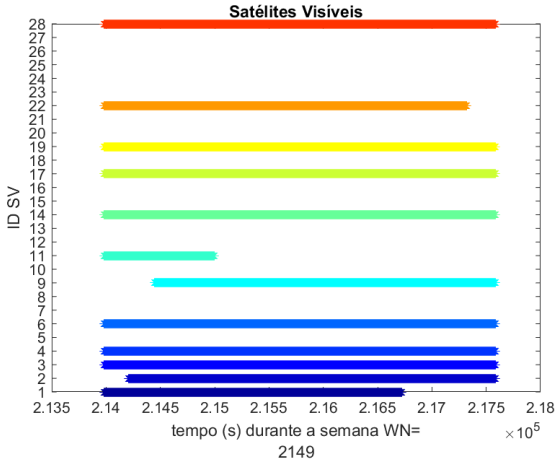

Fig. 12 - Graph of satellite IDs over time

5. CONCLUSIONS

After the elaboration of this project, it is possible to conclude that the tasks initially described as objectives to be overcome were accomplished.

One of the objectives successfully achieved consists in the use, by the simulator, of real orbital parameters of the GPS system and the implementation of models in order to compensate various sources of error affecting the pseudodistance measurements.

A web page was developed for the pseudodistance simulator so that the user has a means through which to interact with the simulator, giving inputs and then receiving various outputs.

As previously mentioned, the user can submit inputs for use by the simulator. This aspect is a benefit for the user since he can manipulate numerous variables of the simulator according to his preferences or scenarios that he wishes to simulate, thus enriching the work developed.

The simulator's outputs consist of the observation RINEX file with the pseudorange of all visible satellites, a plot representing the pseudorange over time, and other similar plots for the tropospheric, ionospheric, and satellite clock drift delay components. In addition to these outputs, the simulator also provides graphs of the DOPs, and graphs of the errors in the receiver position and clock drift estimates. The fact that the user has access to all this information is an added value since it allows not only to obtain pseudoranges according to the data offered to the simulator, but also to draw several conclusions about the factors that affect these same pseudoranges.

The results observed in the operation of the GPS pseudorange simulator are in agreement with the expectations from a theoretical point of view. Thanks to the experiments carried out, it was possible to draw several conclusions about the results obtained. It was possible to observe a relationship between the values of the satellite elevations and the values of the tropospheric and ionospheric delays, the higher the elevations, the lower the delays. It was also concluded that there is a relationship between the DOP values and the number of visible satellites for a given time instant, that is, the greater the number of visible satellites, the lower the value of the DOP parameters. It is also possible to state, given the results of the experiments performed, that the increase in the DOP values corresponds to an increase in the error in the estimates of the position and deviation of the receiver clock. Finally, it was proved that, in simulations with more noise, there is a decrease in the accuracy of the estimates.

6. REFERENCES

[1] "2019 Simulator Buyers Guide". https://www.gpsworld.com/2019-simulator-buyers-guide/ (accessed May 13, 2021).

[2] "2020 Simulator Buyers Guide". https://www.gpsworld.com/2020-simulator-buyers-guide/ (accessed May 13, 2021).

[3] D. Dardari, E. Falletti, e M. Luise, *Satellite and Terrestrial Radio Positioning Techniques: A Signal Processing Perspective*, 1st ed. Waltham, MA, USA: Elsevier, 2012.

[4] A. Leick, L. Rapoport, e D. Tatarnikov, *GPS Satellite Surveying*, 4.th ed. Hoboken, NJ, USA: John Wiley & Sons, Inc., 2015.

[5] A. Küpper, *Location-based Services : Fundamentals and Operation*. 1st ed. West Sussex, England: John Wiley & Sons, Inc., 2005.

[6] A. Flores "NAVSTAR GPS Space Segment/Navigation User Segment Interfaces, Interface Specification IS-GPS-200, Revision M", 2021.

[7] A. LaMarca e E. de Lara, *Location Systems: An Introduction to the Technology Behind Location Awareness*. Bonita Springs, FL, USA: Morgan & Claypool, 2008.

[8] E. D. Kaplan e C. J. Hegarty, *Understanding GPS: Principles and Applications*, 2nd ed. Norwood, MA, USA: Artech House Publishers, 2006.

[9] J. Van Sickle, "PennState College of Earth and Mineral Sciences Official Website: The

Orbital Bias". https://www.e-education.psu.edu/geog862/node/1717 (accessed May 13, 2021).

[10] D. B. Hofmann-Wellenhof, D. H. Lichtenegger, e D. E. Wasle, *GNSS — Global Navigation Satellite Systems: GPS, GLONASS, Galileo, and more*., Viena, Austria: Springer-Verlag Wien, 2008.

[11] J. P. Collins, "Assessment and Development of a Tropospheric Delay Model for Aircraft Users of the Global Positioning System", Department of Geodesy and Geomatics Engineering, University of New Brunswick, Fredericton, Canada, 1999.

[12] J. Van Sickle, "PennState College of Earth and Mineral Sciences Official Website: Receiver Noise". https://www.e-education.psu.edu/geog862/node/1722 (accessed Dec. 16, 2021).

[13] P. Poshala, R. KK, e R. Gupta, "Signal Chain Noise Figure Analysis", *Texas Instruments*, vol. SLAA652, n. October, pp. 1–14, 2014.

[14] J. Sanguino, "Lecture Notes - SPTS". Instituto Superior Técnico, Universidade de Lisboa, 2019 .